ASTM INTERNATIONAL

Geotechnical Testing Journal

T. A. V. Gaspar[1] and S. W. Jacobsz[2]

DOI: 10.1520/GTJ20190078

# Brazilian Tensile Strength Test Conducted on Ductile Unsaturated Soil Samples

Geotechnical Testing Journal

doi:10.1520/GTJ20190078 available online at www.astm.org

# TECHNICAL NOTE

T. A. V. Gaspar[1] and S. W. Jacobsz[2]

# Brazilian Tensile Strength Test Conducted on Ductile Unsaturated Soil Samples

## Reference

T. A. V. Gaspar and S. W. Jacobsz, "Brazilian Tensile Strength Test Conducted on Ductile Unsaturated Soil Samples," *Geotechnical Testing Journal* https://doi.org/10.1520/GTJ20190078

## ABSTRACT

The tensile strength of soil is often neglected. Because of the presence of matric suction, unsaturated soils may have substantial tensile strengths with implications for a range of geotechnical problems, such as slope stability, bearing capacity, and the integrity of clay liners. Direct measurement of the tensile strength of soils is complex to carry out, while the simplicity of the Brazilian tensile strength (BTS) test offers an attractive alternative. However, this method was developed to measure the tensile strength of brittle materials. While suction-bound unsaturated soils may behave in a brittle fashion at low moisture contents, such materials become more ductile as the moisture content increases. This study investigated the application of the BTS test to measure the tensile strength of unsaturated soil samples over a range of moisture contents. Because of the low sample strength of these soils, the use of curved loading platens is recommended. The required load angle depends on the ratio between the compressive and tensile strength of the material tested. When brittle behavior is obtained during testing, conventional interpretation may be used, i.e., the maximum mobilized load during load application is used for tensile strength calculation. This is not appropriate when testing ductile materials. During load application on ductile samples, the initial mobilized load-deformation behavior is approximately linear and becomes nonlinear when tensile yielding starts to occur, originating from the sample center where the full tensile strength is first mobilized. It is recommended that, to obtain a conservative estimate of tensile strength, the inflection point where behavior becomes nonlinear should be taken as representative of soil tensile strength.

## Keywords

tensile strength, unsaturated soil, Brazilian tensile strength test, ductile, brittle

Manuscript received March 5, 2019; accepted for publication March 19, 2020; published online May 18, 2020.

[1] Department of Civil Engineering, University of Pretoria, Lynnwood Rd., Hatfield, Pretoria, 0002, South Africa (Corresponding author), e-mail: tav.gaspar@gmail.com, https://orcid.org/0000-0002-3746-2714

[2] Department of Civil Engineering, University of Pretoria, Lynnwood Rd., Hatfield, Pretoria, 0002, South Africa, https://orcid.org/0000-0002-7439-2276

## Introduction

The tensile strength of uncemented soils is often neglected (Tang and Graham 2000; Yin and Vanapalli 2018). However, surface hydration and capillarity effects can provide significant interparticle tensile strength (Schubert 1975; Snyder and Miller 1985; Kim and Sture 2008; Lu et al. 2009; Akin and Likos 2017b). Depending on factors such as particle size, void ratio, degree of saturation, and relative humidity, the tensile strength of unsaturated soils can range from less than a kilopascal for sands (Lu, Wu, and Tan 2005; Lu et al. 2009) to several hundred kilopascals for clays (Vesga and Vallejo 2006; Stirling et al. 2015). The tensile strength of unsaturated soils is therefore not negligible and finds relevance in many geotechnical applications such as slope stability, bearing capacity, and the integrity of landfill liners (Baker 1981; Thusyanthan et al. 2007; Yin and Vanapalli 2018).

Techniques to measure tensile strength can be divided into direct and indirect methods. Direct tension tests involve uniaxially loading a soil specimen in pure tension and have been researched extensively (Tang and Graham 2000; Heibrock, Zeh, and Witt 2005; Nahlawi, Chakrabarti, and Kodikara 2004; Lu, Wu, and Tan 2005; Kim and Sture 2008; Stirling et al. 2015). Indirect tests involve splitting a soil specimen under a compressive point load or line load, of which the Brazilian disk test is an example (Krishnayya and Eisentein 1974; Ghosh and Subbarao 2006; Beckett et al. 2015; Akin and Likos 2017a, 2017b). Other indirect tests include the double punch test (Fang and Chen 1972; Kim et al. 2007) and bending beam tests (Ajaz and Parry 1975; Thusyanthan et al. 2007).

Akin and Likos (2017a, 2017b) and Krishnayya and Eisenstein (1974) highlighted several advantages of the Brazilian tensile strength (BTS) test over the various direct testing procedures. These include simple specimen geometries, sample preparation, and widely available testing equipment. This allows for many tests to be conducted in a short period of time.

## BTS Test

Originally proposed independently by Carneiro (1943) and Akazawa (1943), the BTS test is a method commonly used to determine the indirect tensile strength of brittle materials such as concrete and rock by loading a disk specimen along its vertical axis to develop tensile stresses perpendicular to the line of load application. The mobilized tensile stress ($\sigma_t$) is typically calculated using the elastic solution proposed by Timoshenko (1934) (equation (1)):

$$\sigma_t = -\frac{2P}{\pi DL} \tag{1}$$

where $P$ is the applied compressive load, $D$ is the disk specimen diameter, and $L$ is the disk thickness.

As the test developed, standards were established for the testing of concrete (BS EN 12390-6:2009, *Testing Hardened Concrete. Tensile Splitting Strength of Test Specimens*; ASTM C496/C496M-17, *Standard Test Method for Splitting Tensile Strength of Cylindrical Concrete Specimens*) and rock (ASTM D3967, *Standard Test Method for Splitting Tensile Strength of Intact Rock Core Specimens*; International Society for Rock Mechanics 1978). Both materials display a brittle response when subjected to loading and, as such, BTS tests performed on these materials can be interpreted in the conventional manner by using the maximum achieved load to calculate the tensile strength. However, as the test is increasingly being used to test materials that may possess some ductility, e.g., fiber-reinforced concrete (FRC) (Denneman, Kearsley, and Visser 2011; Boulekbache et al. 2015) and unsaturated soils (Frydman 1964; Krishnayya and Eisenstein 1974; Vesga and Vallejo 2006; Beckett et al. 2015; Stirling et al. 2015; Akin and Likos 2017a, 2017b), the interpretation of test results for these materials may require further investigation.

A key aspect of the BTS test is that when loading is applied correctly, cracking must initiate in the center of the specimen if the result is to be representative of a tensile failure (Erarslan, Liang, and Williams 2012; Li and

Wong 2013). Despite this crucial condition for the successful implementation of the test, researchers have repeatedly highlighted that this is often not what is observed (e.g., Fairhurst 1964 and Hudson, Brown, and Rummel 1972). Given the possibility of undesired failure mechanisms, it is useful to re-evaluate the stress state imposed on a specimen during a BTS test.

It is generally accepted that the point load $P$ produces a uniform tensile stress distribution along the loaded axis of the sample. However, Denneman, Kearsley, and Visser (2011) pointed out how the use of flat loading strips with finite width results in nonuniform stress distribution, with compressive stress zones occurring near the loading strips. The implications of varying loading conditions can be further investigated using elastic circumferential and radial stress solutions proposed by Hondros (1959) (equations (2) and (3)).

**Figure 1** illustrates a disk specimen loaded by finite arcs and the associated normalized circumferential and radial stress distribution along the depth of a disk specimen, loaded under contact angles of $2\alpha = 10°$ and 30°, respectively.

$$\sigma_\theta = \frac{P}{\pi RL\alpha}\left\{\frac{\left[1-\left(\frac{r}{R}\right)^2\cdot\sin 2\alpha\right]}{1-2\left(\frac{r}{R}\right)^2\cdot\cos 2\alpha+\left(\frac{r}{R}\right)^4}-\tan^{-1}\left[\frac{1+\left(\frac{r}{R}\right)^2}{1-\left(\frac{r}{R}\right)^2}\cdot\tan\alpha\right]\right\} \tag{2}$$

$$\sigma_r = -\frac{P}{\pi RL\alpha}\left\{\frac{\left[1-\left(\frac{r}{R}\right)^2\cdot\sin 2\alpha\right]}{1-2\left(\frac{r}{R}\right)^2\cdot\cos 2\alpha+\left(\frac{r}{R}\right)^4}+\tan^{-1}\left[\frac{1+\left(\frac{r}{R}\right)^2}{1-\left(\frac{r}{R}\right)^2}\cdot\tan\alpha\right]\right\} \tag{3}$$

where $R$ is the disk radius, $r$ is the radial distance from the center of the disk, and $2\alpha$ is the contact angle over which the load is applied.

**Figure 1** demonstrates how reducing the contact angle ($2\alpha$) results in a more uniform distribution of tensile (circumferential) stress within the sample. Reducing the contact angle toward a point load increases the portion of the disk under constant tensile stress. However, this is accompanied by a substantial increase in the compressive

**FIG. 1** (*A*) Disk specimen loaded using curved loading strips and (*B*) normalized circumferential and radial stress distributions along the loaded diameter of a disk specimen.

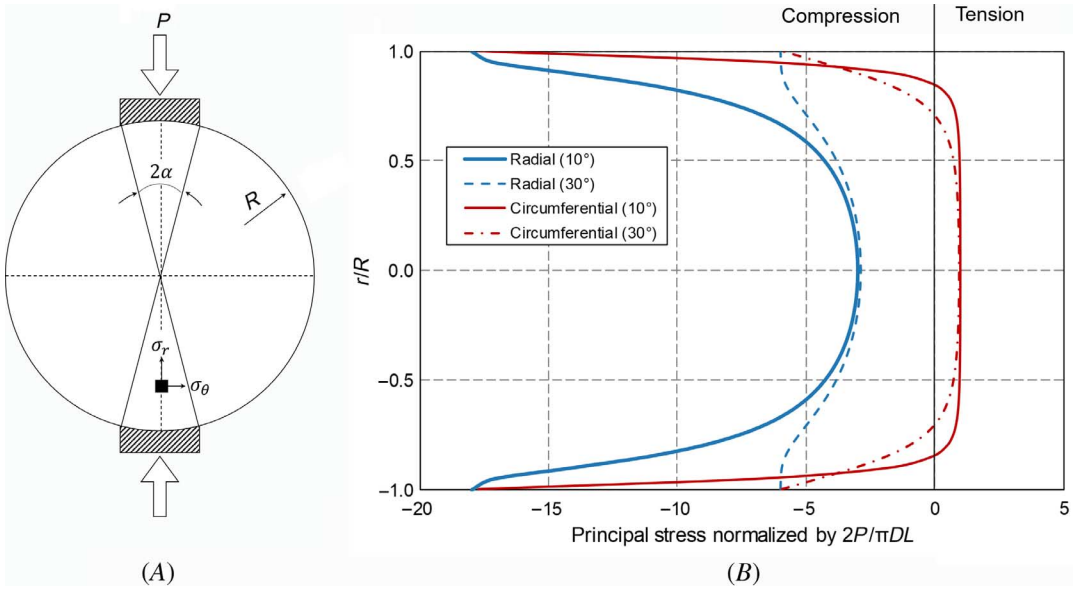

**FIG. 2**

Relationship between contact angle and compressive-to-tensile strength ratio.

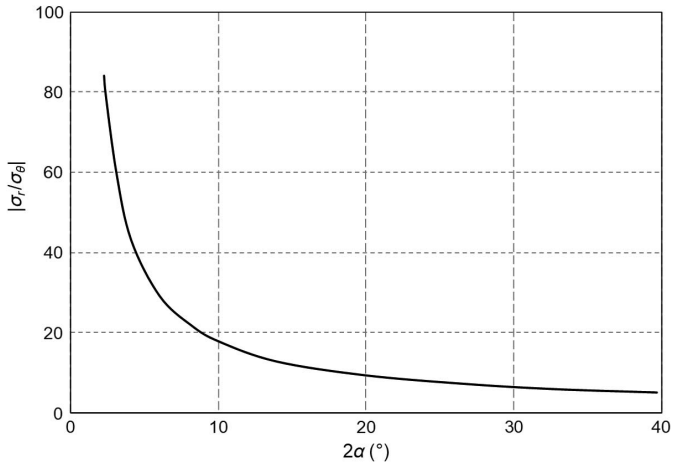


(radial) stresses at the load application points. The ratio of the maximum compressive stress magnitude at the contact point to the maximum tensile stress (at the center of the disk) was found to be as high as 18 for 10° loading arcs compared with just 6.3 for 30° arcs. Furthermore, the use of wider loading arcs does not affect the stress magnitude at the center of the disk where tensile failure first occurs. Using equations (2) and (3), a theoretical relationship can be derived for the ratio of maximum compressive to maximum tensile stresses in the disk as a function of the contact angle $2\alpha$, as presented in **figure 2**.

**Figure 2** shows how for small contact angles ($2\alpha$), the magnitude of compressive stress at the loading platens is many times greater than the tensile stress at the center of the disk. Depending on this ratio, it is possible that the material may be crushed at the sample contacts before tensile failure is induced. Loading strips need to be chosen such that the compressive strength of the material is adequate to withstand the stress concentrations at the loading points, such that the full tensile strength can be mobilized at the center of the specimen. This is especially important when testing weaker materials, such as unsaturated soils.

As the present study focused on the application of the BTS test to weaker and more ductile materials than what is typically tested, a conservative contact angle of 30° was used for this study. **Figure 2** demonstrates that increasing the contact angle further will not significantly reduce the ratio of maximum compressive-to-tensile stresses mobilized within the disk. Furthermore, for this loading condition, the middle third of the sample remains under a uniform tensile stress (**fig. 1*B***). A 30° contact angle was therefore deemed a satisfactory compromise between reducing compressive stress concentrations at the points of load application while preserving a uniform stress distribution along the center portion of the sample.

Displacement-controlled BTS tests were performed in a conventional triaxial test loading frame modified for this purpose. To monitor surface displacements of the sample disks throughout the loading process, digital image correlation (DIC) (White, Take, and Bolton 2003; Stanier et al. 2016) was utilized.

## Materials Tested

Three soils with different particle size distributions (PSDs) and mineralogy were considered in this study, i.e., gold tailings, iron tailings, and transported natural hillwash soil from the Centurion area, south of Pretoria. The respective PSDs and soil water retention curves (SWRCs) are included in **figures 3** and **4**, respectively. The SWRCs presented are all drying curves and are included to present the matric suction magnitudes at which the samples were tested.

**FIG. 3** PSDs of materials tested.

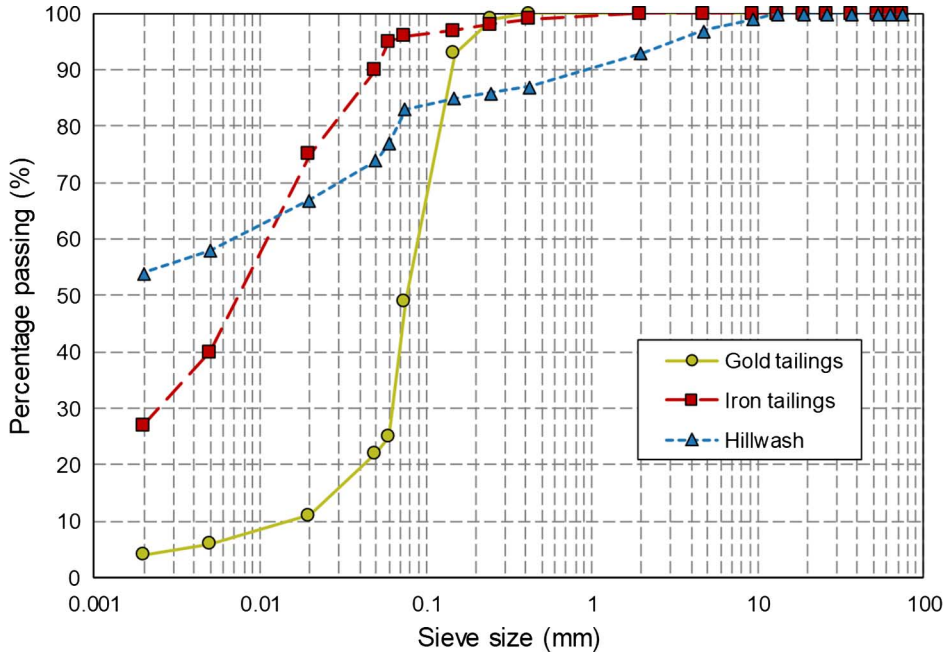


**FIG. 4**

Drying SWRCs of materials tested.

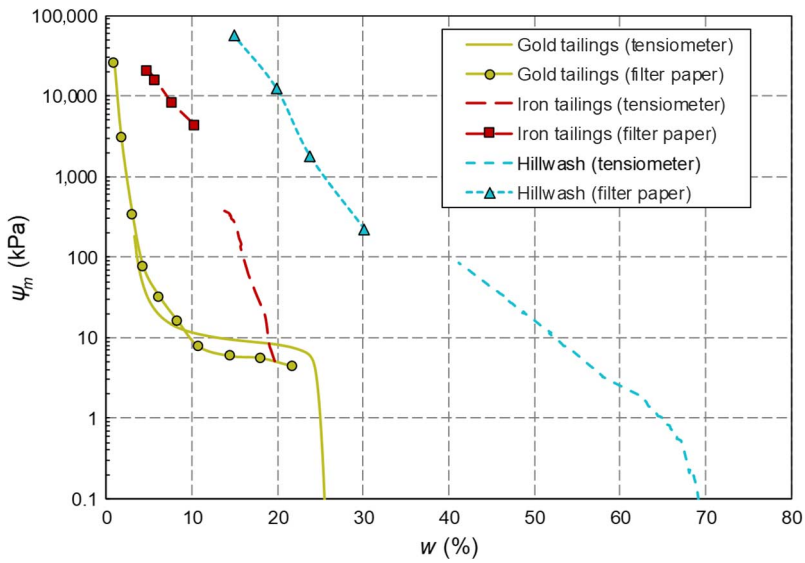


The main mineralogical constituents of the various soils determined by X-ray diffraction were 95 % quartz for the gold tailings and 78 % hematite and 13 % quartz for the iron tailings, with the hillwash soil comprising 33 % quartz, 37 % kaolinite, and 20 % talc. Additional material properties are included in Table 1.

**TABLE 1**
Selected material properties and classification

| Material | Liquid Limit, % | Plastic Limit, % | Plasticity Index, % | $G_s$ | Unified Classification |
|---|---|---|---|---|---|
| Gold tailings | NP | NP | NP | 2.69 | SM |
| Iron tailings | 22 | 14 | 8 | 3.89 | CL |
| Hillwash soil | 67 | 37 | 30 | 2.75 | MH |

*Note*: NP = nonplastic; SM = Silty sand; CL = Clay of low plasticity; MH = Silt of high plasticity.

## Sample Preparation

Samples from each material were prepared from reconstituted pastes, prepared to similar workabilities, and then dried to a range of gravimetric moisture contents. The paste moisture contents were 27, 40, and 60 % for the gold tailings, iron tailings, and hillwash soil, respectively. The paste was deposited into 50-mm-diameter cylindrical molds in 3 layers, each vibrated for 20 s. Specimens were oven dried at 65°C to the desired moisture content. The molds used allowed double drainage to encourage uniform drying. To further facilitate this uniformity, samples were demolded as soon as they could support their own weight. Uniform drying, together with the relatively high density created by vibration, prevented desiccation cracking. At the targeted moisture content, samples were trimmed to a final height of 25 mm. After preparation, samples were sealed and stored for 1 week to allow for moisture content and matric suction equilibration.

## Results

### GOLD TAILINGS

Figure 5 presents calculated tensile stress versus vertical sample compression curves for gold tailings, tested at four different moisture contents, also showing tensile strain development measured using DIC across the width of the sample. The tensile stress was calculated from the mobilized load using equation (1). Being the coarsest of the

**FIG. 5** Mobilized tensile stress and strain during BTS testing of gold tailings samples at various moisture contents. Max. = maximum.

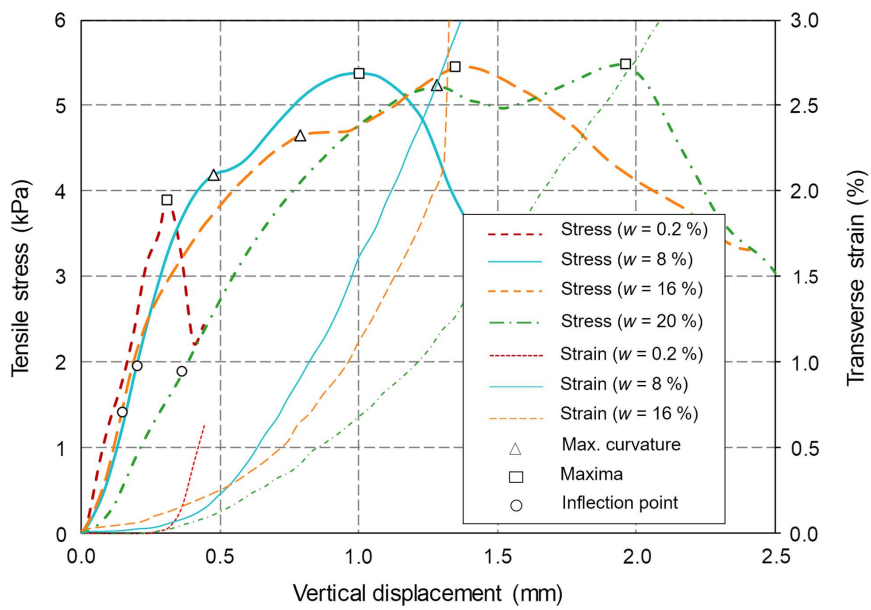

three materials tested, the low matric suction was inadequate to allow stable samples to be prepared at moisture contents close to saturation (i.e., in the capillary regime). The results therefore cover the funicular and pendular regimes.

Following initial contact associated with bedding during load application, the curves of the three wetter samples rose approximately linearly and reached poorly defined inflection points, indicated by the solid disks in **figure 5**. From the inflection points, the slopes of the curves gradually flattened to points of maximum curvature. Following these points, each curve showed a further increase in load, eventually reaching overall peak values.

**Figure 6*A*** presents the tensile stress calculated from the applied load, tested at 8 % moisture content, also showing horizontal tensile strain across the width of the sample. **Figure 6*B*** presents the distribution of horizontal tensile strain along the vertical centerline. **Figure 6*C*** illustrates contour plots of horizontal tensile strain across the sample surface determined using DIC. Comparable results were found for the samples tested at moisture contents of 16 and 20 %.

**Figures 5** and **6*A*** show that the inflection points (Point 1) correspond to the load where horizontal tensile strain began to increase measurably and the stress-compression curve became nonlinear. The tensile stress calculated from this load is referred to herein as the tensile stress at first yield. Up to this point, the magnitude of tensile strains along the sample centerline was negligible (**fig. 6*B***). The nonlinearity following the tensile stress at first yield has also been observed in the testing of concrete and was attributed by Karihaloo (1995) to the progressive formation of microcracking.

**FIG. 6** Strain analysis for gold tailings sample at $w = 8$ % illustrating (*A*) the relationship between tensile stress and transversal strain with respect to vertical compression, (*B*) transverse strain along the sample depth and (*C*) contours of horizontal tensile strain at various stages of testing.

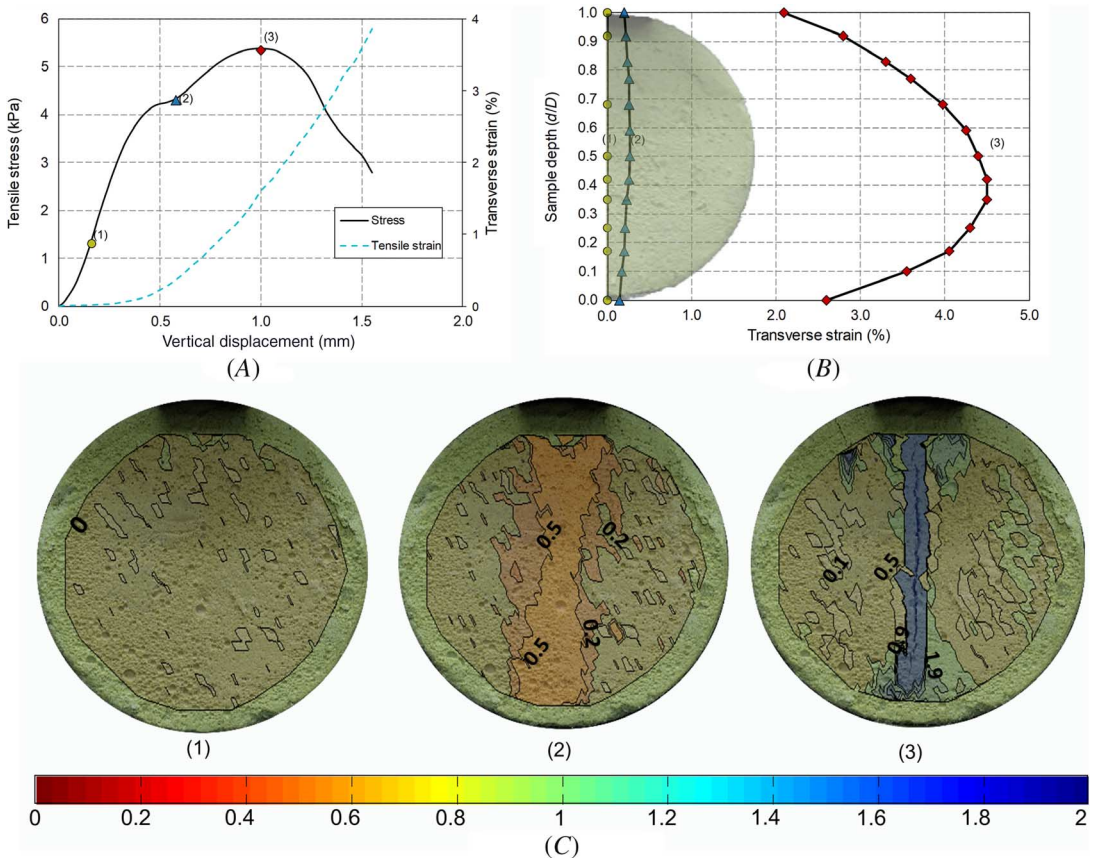

Inflection Point 2 (fig. 6A) coincided with the appearance of a surface crack visible to the naked eye. The crack initiated on the sample centerline where the horizontal strain distribution peaked (fig. 6B). When the surface crack first became visible, the sample had begun to split along its centerline. As the sample was no longer intact beyond this stage, further load supported by the disk was a result of sample compression. The fact that the stress at the second inflection points increased slightly with increasing moisture content is the result of sample barreling, increasing the area resisting the load as the sample deformed, and does not point toward increasing tensile strength.

The peak load (Point 3 in fig. 6A) was reached late in the test as a result of sample compression after it had split, emphasizing the error associated with blindly adopting the maximum applied load to calculate tensile strength in a BTS test conducted on a ductile material.

In contrast to the ductile responses of the wetter samples, distinct brittle behavior was observed for the sample at 0.2 % moisture content. The development of horizontal tensile strain in this test remained insignificant until the peak stress had been reached, after which the sample rapidly split.

## IRON TAILINGS

In contrast to gold tailings, the iron tailings samples developed higher matric suction values in the capillary regime, allowing stable samples to be prepared at high degrees of saturation. However, upon loading, the edges of the loading arcs cut into the samples, deforming them excessively, with no cracking along the vertical axis. These results illustrate an extreme case of sample ductility in which the limitations of BTS testing are obvious and require no further investigation. Iron tailings were tested successfully from the pendular regime ($S_r = 23.0$ %) to the wet side of the funicular regime ($S_r = 65.2$ %).

The tensile stress versus compression curves for the three samples tested are presented in figure 7. The figure illustrates a gradual loss in ductility associated with decreasing saturation. Additionally, curves of horizontal tensile strain are also presented.

While a greater variation in material behavior was observed for iron tailings across the range of moisture contents considered, investigation of the wettest and driest samples revealed trends similar to those for gold tailings. Samples at high degrees of saturation responded in a ductile manner, exhibiting first yield at the early stages of the test, with tensile cracking only becoming visible to the naked eye much later. In contrast, the stress versus

**FIG. 7** Mobilized tensile stress and strain during BTS testing of iron tailings samples at various moisture contents.

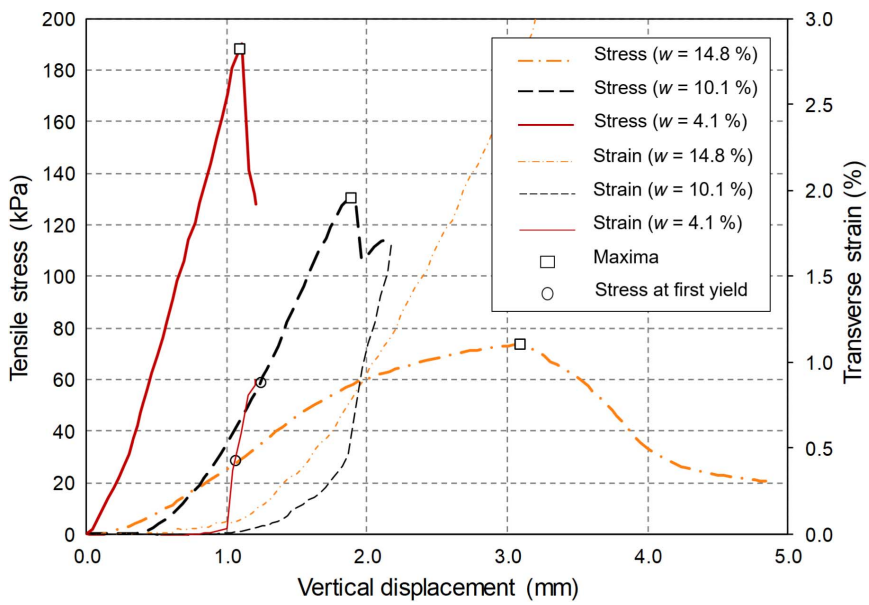

**FIG. 8** Mobilized tensile stress and strain during BTS testing of hillwash samples at (*A*) lower moisture contents and (*B*) higher moisture contents.

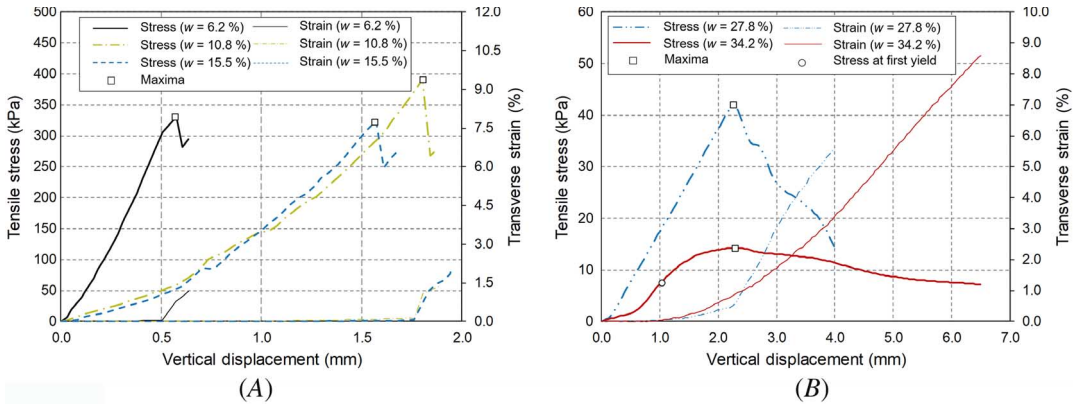


compression curve for the driest sample illustrated an approximately linear response until the peak load was reached. At this point, abrupt splitting failure occurred, accompanied by a sharp increase in horizontal tensile strain. Brittle responses were confined to moisture contents less than the plastic limit ($P_L$), as observed by Stirling et al. (2015).

## HILLWASH SOIL

Figure 8 illustrates the tensile stress versus compression curves for hillwash samples at different moisture contents, also showing horizontal tensile strain. At high degrees of saturation, sample barreling, as encountered for iron tailings, occurred. Nonetheless, the wettest sample was successfully tested at a moisture content of 34 % ($S_r = 92.6$ %), giving an indication of behavior in the capillary regime. Behavior over a wide saturation range could be investigated for the fine-grained hillwash soil.

As for the other materials, the hillwash transitioned from ductile to brittle as moisture content reduced. At high degrees of saturation, sample failure occurred progressively after the onset of microcracking, occurring after the stress at first yield. Tensile failure advanced until a surface crack became visible at the maximum achieved load. In contrast, at lower moisture contents, samples exhibited an approximately linear stress versus compression curve up until a sudden brittle splitting failure occurred. The results of tests conducted on brittle and ductile samples are presented in **figure 8*A*** and **8*B***, respectively. For the hillwash soil, the transition from ductile to brittle behavior occurred as the moisture content was reduced below $0.8P_L$.

## BRAZILIAN TENSILE TEST INTERPRETATION FOR UNSATURATED SOILS

The tendency of an unsaturated soil sample to deform under loading is strongly dependent on the matric suction magnitude in the sample, providing the sample with strength. The matric suction depends on the PSD and degree of saturation and is characterized by the SWRC. The suction magnitudes in fine-grained samples at low degrees of saturation in the pendular regime are high, and the samples are relatively strong and brittle (hillwash soil and iron tailings). More coarse-grained material can also exhibit brittle behavior, but with much lower strength (gold tailings). Upon loading, the stress-compression response of these samples is typically approximately linear, followed by a sharp reduction in strength at tensile failure. An example of such behavior is shown in **figure 9*A***, which also shows tensile strain development. BTS test results from such tests should be interpreted in the usual way by taking the peak applied load to determine tensile strength.

At higher degrees of saturation, typically in the funicular regime, the suction magnitude is much reduced, resulting in weaker, more ductile samples. An example of such behavior during a BTS test is shown in **figure 9*B***.

**FIG. 9** Generic examples of (*A*) brittle and (*B*) ductile load-deformation responses during BTS testing.

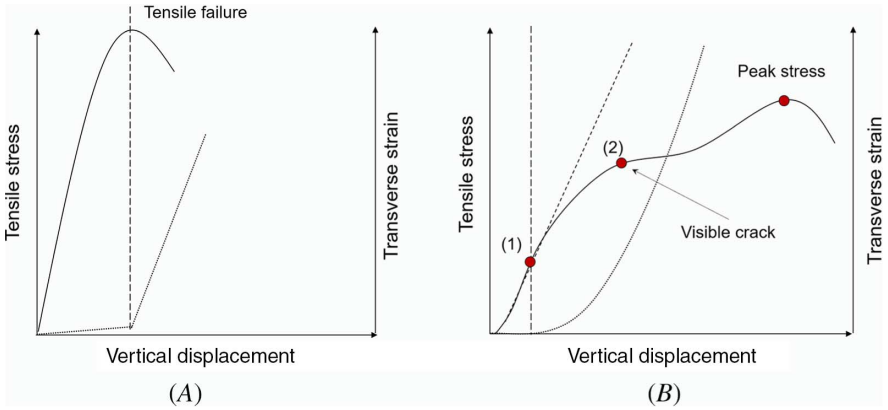


Early concave curvature is typical and is associated with bedding of the loading arcs against the sample. An approximately linear stage progresses until Point 1, at which the tensile strength of the sample is fully mobilized. Beyond this stage, tensile strain increases rapidly as microcracking results in the slope of the curve reducing (as observed by Karihaloo 1995 in concrete). An additional load is supported by sample compression, during which the contribution from tensile strength reduces. At Point 2, the sample is effectively split by a visible crack, and additional applied load is supported by further compression of the sample. A conservative estimate of tensile strength should be determined from the load applied at Point 1, just before the onset of first tensile yielding. At this stage, this disk is still intact, and the elastic solution for the calculation of tensile stress (equation (1)) is most applicable.

Soil samples in the capillary regime were too weak and ductile to be suitable for BTS testing, as the loading arcs punched into the sample and sample barreling occurred. From the moisture contents of samples successfully tested and the corresponding SWRCs, it appears that a minimum matric suction of approximately 20 kPa is required to support samples to allow meaningful BTS tests for the sample geometry presented here.

## Conclusions

Originally intended for the testing of concrete and rock, the simplicity of the BTS test has led to its use in the testing of other materials, such as FRC and unsaturated soils, both of which can exhibit ductile responses. Recognizing that the BTS test was initially intended for the testing of brittle materials, this study investigated BTS test performance when applied to unsaturated soils. The focus was on the appropriate interpretation of BTS test results obtained from ductile materials.

Conventionally, the maximum achieved load applied during a BTS test is used to calculate the ultimate tensile sample strength using the elastic solution by Timoshenko (1934) (equation (1)). This approach is suitable for brittle materials, which typically exhibit steep linear load-deformation behavior up to a maximum value at which sudden failure occurs. Tensile train development prior to this point is negligible.

When testing weak or ductile materials, it is necessary to use curved loading arcs to reduce the compressive contact stresses to prevent premature damage to the sample at the load application points. The appropriate choice of the loading strip contact angles depends on the compressive-to-tensile strength ratio of the material tested. A theoretical relationship is proposed in **figure 2** as a guideline to size the contact angle required. The use of curved loading strips somewhat reduces the uniformity of tensile stresses along the sample centerline but does not alter the magnitude of maximum tensile stress responsible for tensile failure mobilized at the disk center (**fig. 1**).

When testing very ductile materials (e.g., in the capillary regime), the loading plates punch into samples, causing them to barrel, in which case the BTS test is clearly not valid. At reduced moisture contents, ductility

reduces sufficiently to avoid this punching-type sample deformation. When testing such samples, after some initial nonlinear behavior associated with loading platen bedding, the mobilized load increases linearly up to an inflection point. This point is referred to herein as the stress at first tensile yielding. Beyond this point, the mobilized loading rate reduces, and tensile strain development associated with the onset of microcracking (Karihaloo 1995) develops rapidly. With further loading, cracking advances until a maximum applied load is reached.

Beyond first tensile yielding, sample compression becomes progressively more significant so that the mobilized load resistance is not solely related to tensile strength but also related to sample compression.

It is recommended that for ductile materials, the point of first tensile yielding should be adopted as a conservative estimate of tensile strength. Adopting the maximum recorded load to determine the tensile strength of a ductile material can result in a gross overestimation of the indirect tensile strength. The study indicated that the plastic limit provides an initial estimate of the moisture content range below which brittle responses will be observed (i.e., $0 < w < P_L$). However, for the nonplastic gold tailings, brittle behavior was only observed at very low moisture contents.

## References


Ajaz, A. and R. H. G. Parry. 1975. "Stress-Strain Behaviour of Two Compacted Clays in Tension and Compression." *Géotechnique* 25, no. 3 (September): 495–512. https://doi.org/10.1680/geot.1975.25.3.495

Akazawa, T. 1943. "New Test Method for Evaluating Internal Stresses Due to Compression of Concrete: The Splitting Tension Test." *Journal of Japan Society of Civil Engineers* 29: 777–787.

Akin, I. D. and W. J. Likos. 2017a. "Brazilian Tensile Strength Testing of Compacted Clay." *Geotechnical Testing Journal* 40, no. 4 (July): 608–617. https://doi.org/10.1520/GTJ20160180

Akin, I. D. and W. J. Likos. 2017b. "Implications of Surface Hydration and Capillary Condensation for Strength and Stiffness of Compacted Clay." *Journal of Engineering Mechanics* 143, no. 8 (August): 04017054. https://doi.org/10.1061/(ASCE)EM.1943-7889.0001265

ASTM International. 2017. *Standard Test Method for Splitting Tensile Strength of Cylindrical Concrete Specimens*. ASTM C496/C496M–17. West Conshohocken, PA: ASTM International, approved October 1, 2017. https://doi.org/10.1520/C0496_C0496M-17

ASTM International. 2016. *Standard Test Method for Splitting Tensile Strength of Intact Rock Core Specimens*. ASTM D3967–16. West Conshohocken, PA: ASTM International, approved November 1, 2016. https://doi.org/10.1520/D3967-16

Baker, R. 1981. "Tensile Strength, Tension Cracks, and Stability of Slopes." *Soils and Foundations* 21, no. 2 (June): 1–17. https://doi.org/10.3208/sandf1972.21.2_1

Beckett, C. T. S., J. C. Smith, D. Ciancio, and C. E. Augarde. 2015. "Tensile Strengths of Flocculated Compacted Unsaturated Soils." *Géotechnique Letters* 5, no. 4 (December): 254–260. https://doi.org/10.1680/jgele.15.00087

Boulekbache, B., M. Hamrat, M. Chemrouk, and S. Amziane. 2015. "Failure Mechanism of Fibre Reinforced Concrete under Splitting Test Using Digital Image Correlation." *Materials and Structures* 48, no. 8 (August): 2713–2726. https://doi.org/10.1617/s11527-014-0348-x

British Standards Institution. 1983. *Testing Hardened Concrete. Tensile Splitting Strength of Test Specimens*. BS EN 12390-6:2009. London: British Standards Institution.

Carneiro, F. L. L. B. 1943. "A New Method to Determine the Tensile Strength of Concrete." In *Proceedings of the Fifth Meeting of the Brazilian Association for Technical Rules*, 126–129. Sao Paulo, Brazil: Brazilian Association of Technical Standards.

Denneman, E., E. P. Kearsley, and A. T. Visser. 2011. "Splitting Tensile Test for Fibre Reinforced Concrete." *Materials and Structures* 44, no. 8 (October): 1441–1449. https://doi.org/10.1617/s11527-011-9709-x

Erarslan, N., Z. Z. Liang, and D. J. Williams. 2012. "Experimental and Numerical Studies on Determination of Indirect Tensile Strength of Rocks." *Rock Mechanics and Rock Engineering* 45, no. 5 (September): 739–751.

Fairhurst, C. 1964. "On the Validity of the 'Brazilian' Test for Brittle Materials." *International Journal of Rock Mechanics and Mining Sciences & Geomechanical Abstracts* 1, no. 4 (October): 535–546. https://doi.org/10.1016/0148-9062(64)90060-9

Fang, H. Y. and W. F. Chen. 1972. *Further Study of Double-Punch Test for Tensile Strength of Soils, 348.6*. Bethlehem, PA: Lehigh University.

Frydman, S. 1964. "The Applicability of the Brazilian (Indirect Tension) Test to Soils." *Australian Journal of Applied Science* 15, no. 4: 335–343.

Ghosh, A. and C. Subbarao. 2006. "Tensile Strength Bearing Ratio and Slake Durability of Class F Fly Ash Stabilized with Lime and Gypsum." *Journal of Materials in Civil Engineering* 18, no. 1 (February): 18–27. https://doi.org/10.1061/(ASCE)0899-1561(2006)18:1(18)

Heibrock, G., R. M. Zeh, and K. J. Witt. 2005. "Tensile Strength of Compacted Clays." In *Unsaturated Soils: Experimental Studies*, 395–412. Berlin, Germany: Springer-Verlag.

Hondros, G. 1959. "The Evaluation of Poisson's Ratio and the Modulus of Materials of a Low Tensile Resistance by the Brazilian (Indirect Tensile) Test with Particular Reference to Concrete," *Australian Journal of Applied Science* 10, no. 3: 243–268.

Hudson, J. A., E. T. Brown, and F. Rummel. 1972. "The Controlled Failure of Rock Disks and Rings Loaded in Diametral Compression." *International Journal of Rock Mechanics and Mining Sciences & Geomechanics Abstracts* 9, no. 2 (March): 241–244. https://doi.org/10.1016/0148-9062(72)90025-3

International Society for Rock Mechanics. 1978. "Suggested Methods for Determining Tensile Strength of Rock Materials." *International Journal of Rock Mechanics and Mining Sciences & Geomechanics Abstracts* 15, no. 3 (June): 99–103. https://doi.org/10.1016/0148-9062(78)90003-7

Karihaloo, B. L. 1995. *Fracture Mechanics & Structural Concrete*. Harlow, UK: Longman Scientific & Technical.

Kim, T. H., C. K. Kim, S. J. Jung, and J. H. Lee. 2007. "Tensile Strength Characteristics of Contaminated and Compacted Sand-Bentonite Mixtures." *Environmental Geology* 52, no. 4 (April): 653–661. https://doi.org/10.1007/s00254-006-0494-8

Kim, T.-H. and S. Sture. 2008. "Capillary-Induced Tensile Strength in Unsaturated Sands." *Canadian Geotechnical Journal* 45, no. 5 (May): 726–737. https://doi.org/10.1139/T08-017

Krishnayya, A. V. G. and Z. Eisenstein. 1974. "Brazilian Tensile Test for Soils." *Canadian Geotechnical Journal* 11, no. 4 (November): 632–642. https://doi.org/10.1139/t74-064

Li, D. and L. N. Y. Wong. 2013. "The Brazilian Disc Test for Rock Mechanics Applications: Review and New Insights." *Rock Mechanics and Rock Engineering* 46, no. 2 (March): 269–287. https://doi.org/10.1007/s00603-012-0257-7

Lu, N., T.-H. Kim, S. Sture, and W. J. Likos. 2009. "Tensile Strength of Unsaturated Sand." *Journal of Engineering Mechanics* 135, no. 12 (December): 1410–1419. https://doi.org/10.1061/(ASCE)EM.1943-7889.0000054

Lu, N., B. Wu, and C. P. Tan. 2005. "A Tensile Strength Apparatus For Cohesionless Soils," *Advanced Experimental Unsaturated Soil Mechanics*, edited by A. Tarantino, E. Romero, and Y. J. Cui, 105–110. London: Taylor & Francis.

Nahlawi, H., S. Chakrabarti, and J. Kodikara. 2004. "A Direct Tensile Strength Testing Method for Unsaturated Geomaterials." *Geotechnical Testing Journal* 27, no. 4 (July): 356–361. https://doi.org/10.1520/GTJ11767

Schubert, H. 1975. "Tensile Strength of Agglomerates." *Powder Technology* 11, no. 2 (March–April): 107–119. https://doi.org/10.1016/0032-5910(75)80036-2

Snyder, V. A. and R. D. Miller. 1985. "Tensile Strength of Unsaturated Soils." *Soil Science Society of America Journal* 49, no. 1 (January–February): 58–65. https://doi.org/10.2136/sssaj1985.03615995004900010011x

Stanier, S. A., J. Blaber, W. A. Take, and D. J. White. 2016. "Improved Image-Based Deformation Measurements for Geotechnical Applications." *Canadian Geotechnical Journal* 53, no. 5 (May): 727–739. https://doi.org/10.1139/cgj-2015-0253

Stirling, R. A., P. Hughes, C. T. Davie, and S. Glendinning. 2015. "Tensile Behaviour of Unsaturated Compacted Clay Soils — A Direct Assessment Method." *Applied Clay Science* 112–113 (August): 123–133. https://doi.org/10.1016/j.clay.2015.04.011

Tang, G. and J. Graham. 2000. "A Method for Testing Tensile Strength in Unsaturated Soils." *Geotechnical Testing Journal* 23, no. 3 (September): 377–382. https://doi.org/10.1520/GTJ11059J

Thusyanthan, N. I., W. A. Take, S. P. G. Madabhushi, and M. D. Bolton. 2007. "Crack Initiation in Clay Observed in Beam Bending." *Géotechnique* 57, no. 7 (September): 581–594. https://doi.org/10.1680/geot.2007.57.7.581

Timoshenko, S. 1934. *Theory of Elasticity*. New York: McGraw-Hill.

Vesga, L. F. and L. E. Vallejo. 2006. "Direct and Indirect Tensile Tests for Measuring the Equivalent Effective Stress in a Kaolinite Clay." In *Unsaturated Soils 2006*, 1290–1301. Reston, VA: American Society of Civil Engineers.

White, D. J., W. A. Take, and M. D. Bolton. 2003. "Soil Deformation Measurement Using Particle Image Velocimetry (PIV) and Photogrammetry." *Géotechnique* 53, no. 7 (September): 619–631. https://doi.org/10.1680/geot.2003.53.7.619

Yin, P. and S. K. Vanapalli. 2018. "Prediction of Tensile Strength on Compacted Soils: A Review." In *Proceedings of the Seventh International Conference on Unsaturated Soils*. London: International Society for Soil Mechanics and Geotechnical Engineering.